Journal of Membrane Science 390–391 (2012) 211–217

Contents lists available at SciVerse ScienceDirect

Journal of Membrane Science

journal homepage: www.elsevier.com/locate/memsci

# Important factors influencing molecular weight cut-off determination of membranes in organic solvents

H.J. Zwijnenberg[a,*,1], S.M. Dutczak[a,b,1], M.E. Boerrigter[a], M.A. Hempenius[c], M.W.J. Luiten-Olieman[d], N.E. Benes[b], M. Wessling[b,2], D. Stamatialis[e]

[a] European Membrane Institute – Twente, MESA+ Institute for Nanotechnology, University of Twente, P.O. Box 217, NL-7500 AE Enschede, The Netherlands
[b] Membrane Science and Technology, MESA+ Institute for Nanotechnology, University of Twente, P.O. Box 217, NL-7500 AE Enschede, The Netherlands
[c] Materials Science and Technology of Polymers, MESA+ Institute for Nanotechnology, University of Twente, P.O. Box 217, NL-7500 AE Enschede, The Netherlands
[d] Inorganic Membranes, MESA+ Institute for Nanotechnology, University of Twente, P.O. Box 217, NL-7500 AE Enschede, The Netherlands
[e] Biomaterials Science & Technology, MIRA Institute for Biomedical Technology and Technical Medicine, University of Twente, P.O. Box 217, NL-7500 AE Enschede, The Netherlands

ARTICLE INFO

*Article history:*
Received 6 June 2011
Received in revised form
27 September 2011
Accepted 21 November 2011
Available online 30 November 2011

*Keywords:*
Solvent resistant nanofiltration
MWCO characterization
Flow-induced polymer deformation
Polystyrene
Polyisobutylene

ABSTRACT

In solvent resistant nanofiltration (SRNF), sensible selection of a membrane for a particular solvent/solute system is recognized as challenging. Prospective methods for suitability analysis of membranes include molecular weight cut off (MWCO) characterization. However, insufficient understanding of the interrelated effects of solvent, solute, membrane properties, and the applied process conditions often complicates interpretation of MWCO data. This study demonstrates and discusses such effects with respect to transport mechanism. To this end very different SRNF systems have been selected: a rigid porous membrane (hydrophobized zirconia) versus a rubbery dense membrane (polydimethylsiloxane); a low flux solvent (toluene) versus high flux solvent (n-hexane); and a stiff solute (polystyrene) versus a flexible solute (polyisobutylene). The results indicate that, for the applied conditions, the MWCO of the dense membrane is predominantly affected by solute–membrane and solvent–membrane interactions. For the rigid porous membrane a significant effect of applied pressure is observed, in particular for the flexible solute. The non-linear relation between flux and pressure and the variations in MWCO with pressure indicate combined effects of concentration polarization and shear induced deformation of the flexible solute. The results unmistakably show that the interpretation of MWCO is heavily dependent on the system under study.



## 1. Introduction

In solvent resistant nanofiltration (SRNF) recently significant improvements have been achieved in the development of solvent stable membranes [1,2]. An increasing number of successful applications have been reported in catalysis, the petrochemical industry and pharmaceutical industry. These applications include recovery of solvents (e.g. toluene) from dewaxed lube oil filtrates [3], solvent exchange [4], recovery of the organometallic complexes from various organic solvents [5], separation of phase transfer catalyst (PTC) from toluene [6,7], deacidification of vegetable oils [8,9] and concentration of pharmaceuticals [10–12].

Amongst others, application of SRNF membranes is hampered by the complications involved in selecting appropriate membranes for each distinct separation [12]. The choice for a particular membrane can be based on its MWCO, however, MWCO analysis in SRNF is less developed and more complicated as compared to aqueous systems [13–20]. The complexity of MWCO in SRNF arises from pronounced effects of process conditions, inherent properties of the membrane, and solvent–solute–membrane interactions.

Currently there is no universal protocol for determining the MWCO of SRNF membranes. A promising method is the filtration of a mixture of a homologues series of neutral polystyrene oligomers in toluene, as proposed by Voigt et al. [21]. This method was systematically further developed by Zwijnenberg [22], See Toh et al. [23] and Dutczak et al. [24]. Based on this approach, the present work investigates the effect of process conditions and the interrelated and inherent properties of different components. To this end, different SRNF systems have been selected:

- Membrane: rigid and porous (zirconia) versus rubbery and dense (polydimethylsiloxane).

* Corresponding author. Tel.: +31 053 4893674; fax: +31 053 4894611.
*E-mail address:* h.j.zwijnenberg@utwente.nl (H.J. Zwijnenberg).
[1] Both authors contributed equally to this paper.
[2] Present address: Chemische Verfahrenstechnik (CVT), RWTH Aachen University, 52064 Aachen, Germany.

0376-7388/$ – see front matter © 2011 Elsevier B.V. All rights reserved.
doi:10.1016/j.memsci.2011.11.039

- Solvent: low flux (toluene) versus high flux (n-hexane).
- Solute: stiff solute (polystyrene) versus a flexible solute (polyisobutylene).

The choice of membranes represents two extremes in SRNF. Solvent fluxes through the porous membrane will be much higher as compared to the dense membrane. Consequently, for the porous membrane, concentration polarization effects and shear-induced deformation of the solutes [25] are expected to be more pronounced. In contrast to the rigid porous membrane, the rubbery dense membrane can exhibit pronounced swelling due to sorption of the solvent. Solvent selection is based on anticipated differences in flux. Compared to toluene, higher fluxes have been observed for n-hexane [16–18,26] corresponding to more pronounced effects of flow-induced solute deformation and concentration polarization. In addition, solvent–solute interactions will be different. Selected solutes, polystyrene (PS) and polyisobutylene (PIB) are homologous oligomer mixtures, allowing for a broad molecular weight distribution. Crucial differences between these solutes are their shape and flexibility; compared to PS, PIB can be considered a long thin and flexible molecule [27].

This study aims at giving a practical display of the effects on the found MWCO originating from:

- Process conditions and phenomena such as concentration polarization.
- Interactions between solvent, solute, and membrane.
- Shape and flexibility of solute.

In that respect it shows the difference in transport behavior of the solutions rather than characterizing the membranes themselves.

## 2. Experimental

### 2.1. Materials

Toluene, n-hexane, methanol and tetrahydrofuran (THF), all analytical grades, were purchased from Merck (The Netherlands). Styrene (Reagent Plus ≥99%) and sec-butyllithium solution (1.4 M in cyclohexane) were purchased from Sigma–Aldrich (The Netherlands). The polyisobutylene (PIB), Glissopal® of 550, 1000, 1300, and 2300 g/mol were kindly provided by BASF – Germany and the PIB of 350 g/mol by Janex S.A. – Switzerland. All chemicals were used as supplied without additional purification. General Electric polydimethylsiloxane (PDMS) RTV 615 kit was purchased from Permacol B.V. (The Netherlands). A two component epoxy resin Araldite® 2014-1 obtained from Viba (The Netherlands) was used as potting for modules containing PDMS/α-alumina HF composite membranes. Powders used for preparation of the hollow fiber α-alumina support were AKP 15 (particle size 0.6 μm) and AKP 50 (particle size 0.2 μm) purchased from Sumitomo Chemicals Co. Ltd. Poly(ethersulfone) (PES, Ultrason, 6020P) was used as polymer binder, N-methylpyrrolidone (NMP, 99.5% (w/w), Aldrich) as solvent, deionized water as non-solvent. The α-alumina powder and PES were dried before use; all other chemicals were used without further treatment. A commercial multichannel porous silanized zirconia membrane, referred to as zirconia, was kindly supplied by Fraunhofer-Institut für Keramische Technologien und Systeme – IKTS (former HITK, Hermsdorf, Germany). The selective layer of this membrane was produced by formation of a thin sol–gel derived zirconia coating with a pore size of 3 nm, followed by silanization to form a hydrophobic surface. The resulting pore size was therefore well below the 3 nm resulting in a membrane with true NF properties.

**Table 1**
Spinning dope compositions for the fabrication of the alumina support.

| Spinning dope | Composition, % (w/w) | | | | | |
|---|---|---|---|---|---|---|
| | PES | NMP | AKP 15 | AKP 50 | $H_2O$ | PVP |
| Inner (support layer) | 10 | 39 | 49 | – | – | 2 |
| Outer (separating layer) | 12 | 52 | – | 33 | 3 | 0 |

### 2.2. Composite hollow fiber membrane preparation

#### 2.2.1. Preparation of an α-alumina hollow fiber support

Hollow fibers were prepared via a dry–wet spinning process followed by heat treatment, as described in detail elsewhere [28]. Two spinning mixtures were prepared for the preparation of the inner and the outer layer (see Table 1). The alumina powder was added to a NMP or in a NMP/$H_2O$ mixture followed by stirring for 15 min and ultrasonic treatment for 15 min to decrease the amount of agglomerates in the alumina powder. PES was added in three steps with a time interval of 2 h followed by stirring overnight. The NMP/PES ratio was kept constant (4/1), while the concentration of α-alumina was varied. The concentration of α-alumina particles was lowered in spinning mixture of the outer layer to achieve a thinner layer and water was added to improve the morphology of the layer. Prior to spinning the mixtures were degassed by applying vacuum for 30 min and left for 16 h under dry air.

Spinning experiments were performed with a bore liquid flow of 7 ml/min, air gap of 3 cm and pressure differences of 1 and 2.5 bars for the inner and outer layer, respectively. The spinning mixtures (see Table 1) were pressurized in a stainless steel vessel, and consequently pressed through a spinneret (inner and outer diameter of 0.8 mm/2.0 mm for inner layer and 2.2 mm/2.5 mm for outer layer). After spinning, the fiber was immersed in a water bath for further solvent exchange for 1 day followed by drying and stretching (0.5 cm/m) for 1 day to straighten the fiber. The removal of PES was performed at 400 °C for 120 min (heating rate 1 °C $min^{-1}$) and the fibers were sintered at 1500 °C for 300 min (heating rate 1 °C $min^{-1}$, cooling rate 5 °C $min^{-1}$) in air.

#### 2.2.2. PDMS coating on an α-alumina hollow fiber support

Composite α-alumina/PDMS hollow fiber membranes (referred to here as PDMS membranes) were prepared in an ISO-6 class dust free room. The membranes were prepared by dip-coating in the 3.2% (w/w) pre-crosslinked PDMS/toluene solution of viscosity 175 MPa sat the outside of the fiber. Pre-crosslinking was carried out in order to prevent significant pore intrusion of the PDMS in the support. The coating was performed using an automated set-up adjusted to an immersion/pull up velocity of 0.9 cm/s and a contact time of 30 s. The pre-crosslinked PDMS coating solution was prepared in three steps, starting from 15% (w/w) PDMS solution in toluene. First, the solution was crosslinked at 60 °C for 150 min then at 50 °C till it reached 100 MPa s viscosity. In the next step, it was diluted to 7.5% (w/w) and the reaction continued at 60 °C till again the solution reached 100 MPa s viscosity. Finally, the solution was diluted to 3.2% (w/w) and brought to a viscosity of 175 MPa s by crosslinking at 60 °C. Detailed descriptions of pre-crosslinking of the PDMS solution as well as the coating procedure can be found elsewhere [24].

#### 2.2.3. HF Module preparation

The composite PDMS membranes were potted in cross-flow stainless steel modules. Each module contained one fiber of 155 mm active length. Araldite® 2014-1 was used as a potting material. The resin was allowed to set at room temperature for minimum 24 h before using the module for permeation experiments.

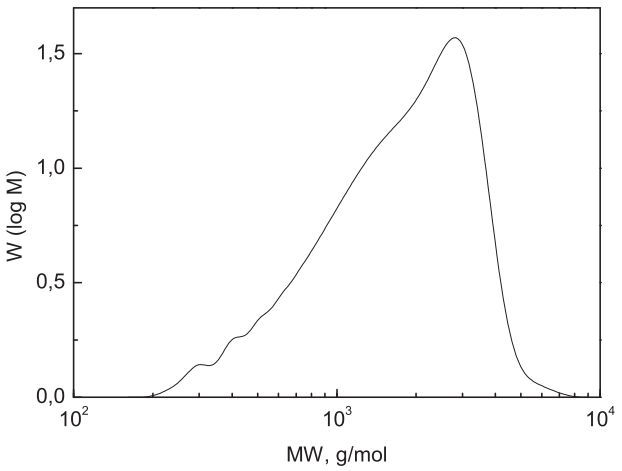


**Fig. 1.** Molecular weight distribution of the synthesized polystyrene.

### 2.3. MWCO determination

#### 2.3.1. Polystyrene synthesis

PS of broad molecular weight distribution 300–6000 g/mol was synthesized by anionic living polymerization in a similar way as described in prior work [24] but with intermediate termination of part of the living chains.

In the reaction flask, containing toluene (500 g), 1.4 M *sec*-butyllithium (200 ml, 0.28 mol) was injected through the septum. The subsequent addition of a toluene–styrene solution to the *sec*-butyllithium dissolved in toluene was performed in three steps:

(1) Styrene (42.8 g, 0.41 mol) in toluene (90 g) was added within 2 min. After 5 min of stirring, MeOH (1.1 ml, 0.03 mol) was injected into the reaction solution in order to quench 10% of growing chains.
(2) Styrene (228.1 g, 2.18 mol) and MeOH (9.4 ml, 0.23 mol) in toluene (480 g) was added dropwise during 3 h 45 min into the polymerization mixture.
(3) Directly afterwards, styrene (14.3 g, 0.14 mol) dissolved in toluene (30 g) was added within 1 min to the polymerization solution. The temperature of the reaction mixture was maintained below 30 °C at all times. The polymer solution was stirred for an additional 2 h at room temperature and quenched with methanol (4 ml).

The resulting oligomer mixture had an average MW of about 1950 g/mol, see Fig. 1 for the GPC results.

In order to ensure a sufficient concentration of low and high MW fractions of PS, the synthesized PS was mixed together in 1:1:1 (w/w) ratio with a PS batch of 1000 g/mol and one of 10,000 g/mol PS. The synthesis of these latter batches is described elsewhere [24]. This particular mixture, of 200–20,000 g/mol, was chosen to obtain the rejection behavior of the membranes above 1000 g/mol and check for leakages.

#### 2.3.2. Permeation experiments

All permeation experiments were performed in a custom made cross-flow high pressure permeation set-up [24]. The set-up was equipped with a pressure and a circulation pump to adjust both pressure and circulation speed independently of each other. All permeation experiments were performed in a total recycle mode at a cross-flow velocity of the feed solution of 2.4 m/s for the PDMS composite membrane and 4.0 m/s for the zirconia membrane. These velocities corresponded to Reynolds numbers of approximately 20,000 for toluene and 31,000 for hexane and a stage cut below 1%. The temperature of the feed solution was controlled at 25 °C. All zirconia permeation experiments were performed using one module of $626.7 \times 10^{-4}$ m$^2$. Each measurement was performed in triplicate. For the PDMS permeation studies we used three membrane modules of $7.1 \times 10^{-4}$ m$^2$, each. The average of the three membranes is reported here.

Before starting the flux or MWCO measurement, each membrane module was pressurized at the test pressure for minimum 2 h to reach the steady state conditions. The permeance coefficient, $P$ (l m$^{-2}$ h$^{-1}$ bar$^{-1}$), was calculated from the slope of the flux ($J$, in l m$^{-2}$ h$^{-1}$) versus trans membrane pressure (TMP) graph. Determination of the pure solvent permeance coefficients was always carried out first. Afterwards, the permeation of 0.3% (w/w) PS mixture, with MW distribution ranging from 300 to 20,000 g/mol, was performed in order to obtain MWCO curves. Next a PIB mixture of 1:1:1:1:1 (w/w) of five fractions: 350, 550, 1000, 1300, and 2300 g/mol, all having a broad MW distribution, was dissolved in toluene at a total polymer concentration of 0.3% (w/w). The resulting PIB oligomer mixture had a MW ranging from 200 to 20,000 g/mol. It was used to determine MWCO curves for all tested membranes in the toluene–PIB system. The same composition and concentration of PIB was used for tests in the n-hexane–PIB system. In order to ensure that the separation performance of the membranes was not changed during filtration experiments, permeation of PS–toluene solution was repeated and compared to the initial results. The concentration of PS and PIB oligomers in the feed and permeate stream was determined by GPC chromatography. For PS a PSS SDV 1000 Å column was used with analytical grade toluene as a mobile phase. In the case of PIB, tandem columns PSS SDV 100 Å and PSS SDV 1000 Å were used with analytical grade THF as a mobile phase. The GPC analysis is described in detail elsewhere [24].

## 3. Results and discussion

### 3.1. PDMS membrane fabrication

Fig. 2 presents SEM images of the cross section of the composite PDMS/α-alumina membrane. The outer diameter of the fiber was ~1.5 mm and the wall thickness ~0.28 mm. The cross section image reveals a distinct PDMS layer on a support consisting of two α-alumina layers with different particle size. The layers adhere very well. The inner α-alumina layer has relatively large pores in between particles combined with a noticeable macrovoid volume, corresponding to low resistance to mass transport. The outer α-alumina layer exhibits less macrovoids and has smaller interparticle pores, to prevent infiltration of the PDMS top layer. Dutczak et al. [24] described the importance of having small pores in the top layer of the support. The thickness of the PDMS layer was estimated to be $6 \pm 1$ μm with pore intrusion ~2 μm, using a procedure described elsewhere [24].

### 3.2. Membrane permeance and MWCO

#### 3.2.1. Effects of the solute

Fig. 3a presents the flux of pure toluene and PS/toluene and PIB/toluene mixtures as function of pressure for both membranes whereas Fig. 3b and c presents the PS and PIB retention curves of the membranes. Please note that whereas in Fig. 3a the symbols represent actual experimental values, the symbols in Fig. 3b and c only serve to guide the eye between the different lines resulting from the gel permeation chromatograph analysis.

For the PDMS composite membrane there is a linear relation between toluene flux and pressure that is not significantly affected by the presence of PS or PIB (Fig. 3a). The membrane

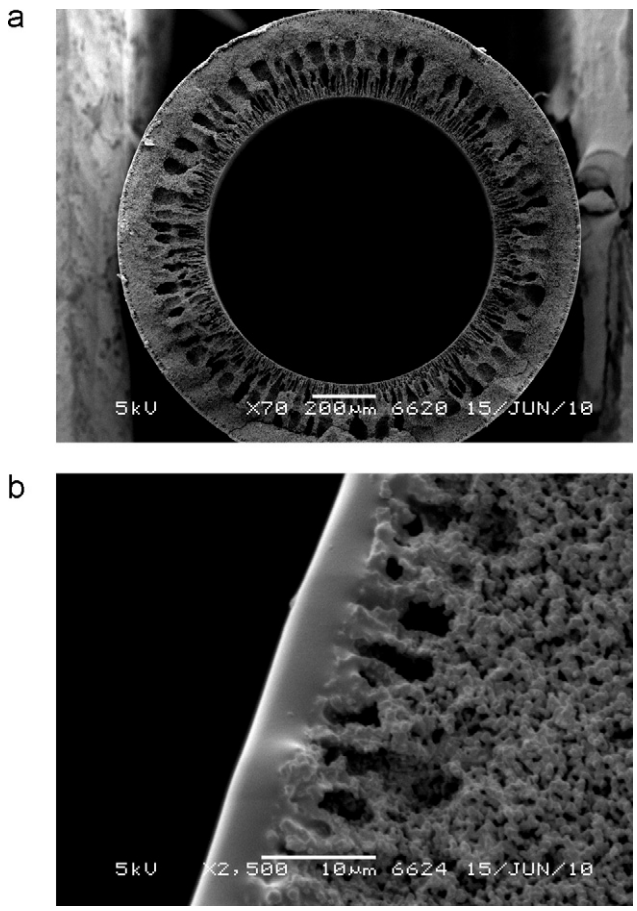


**Fig. 2.** SEM pictures of composite α-alumina/PDMS hollow fiber: (a) Cross-section (magnification 75×) and (b) cross-section (magnification 2500×).

permeance coefficient is relatively low ($P_{tol}$ = 1.1, l m$^{-2}$ h$^{-1}$ bar$^{-1}$). The PS and PIB retention curves of PDMS (Fig. 2b) reveal that the MWCO obtained with PIB is almost double (900 g/mol) as compared to that obtained with PS (500 g/mol). Since the flux through the PDMS membrane is unaffected by the presence of the solutes and the extent of membrane swelling is dominated by the solvent (the toluene volume fraction in the membrane is $\Phi_{toluene}$ = 0.73 [26]), the difference in retention must be a consequence of differences in molecular properties of the solutes. The lower retention of PIB is probably due to a combination of higher solubility and higher diffusivity in the membrane. A higher solubility can be justified based on the small difference between solubility parameters of PIB and PDMS ($\Delta\delta_{PDMS\text{-}PIB} \approx 0.4$), as compared PS and PDMS ($\Delta\delta_{PDMS\text{-}PS} \approx 3.0$–$2.3$ MPa$^{1/2}$) [29,30].

It can be noted that although this highly swollen membrane consists for almost 3/4 of toluene, the larger radius of gyration for PIB in toluene, does not result in a higher retention. Apparently, the interaction of the solute with the PDMS network still dominates the transport.

A higher diffusivity can be expected based on the smaller chain diameter and higher flexibility of PIB in comparison to PS [31], see Table 2. The smaller and more flexible PIB will be more mobile in the swollen PDMS, which according to Tarleton et al. could even be envisioned as an ill-defined porous structure with the pore size in the range of 1.0–1.5 nm [34,35].

Fig. 3b shows that there is no influence of pressure on the retention of PIB and PS oligomers by the PDMS composite membrane, similar to earlier observations [24]. This is a strong indication that the fluxes of solvent and solute through the PDMS are not directly coupled, i.e., via a solvent–solute friction term probably due to

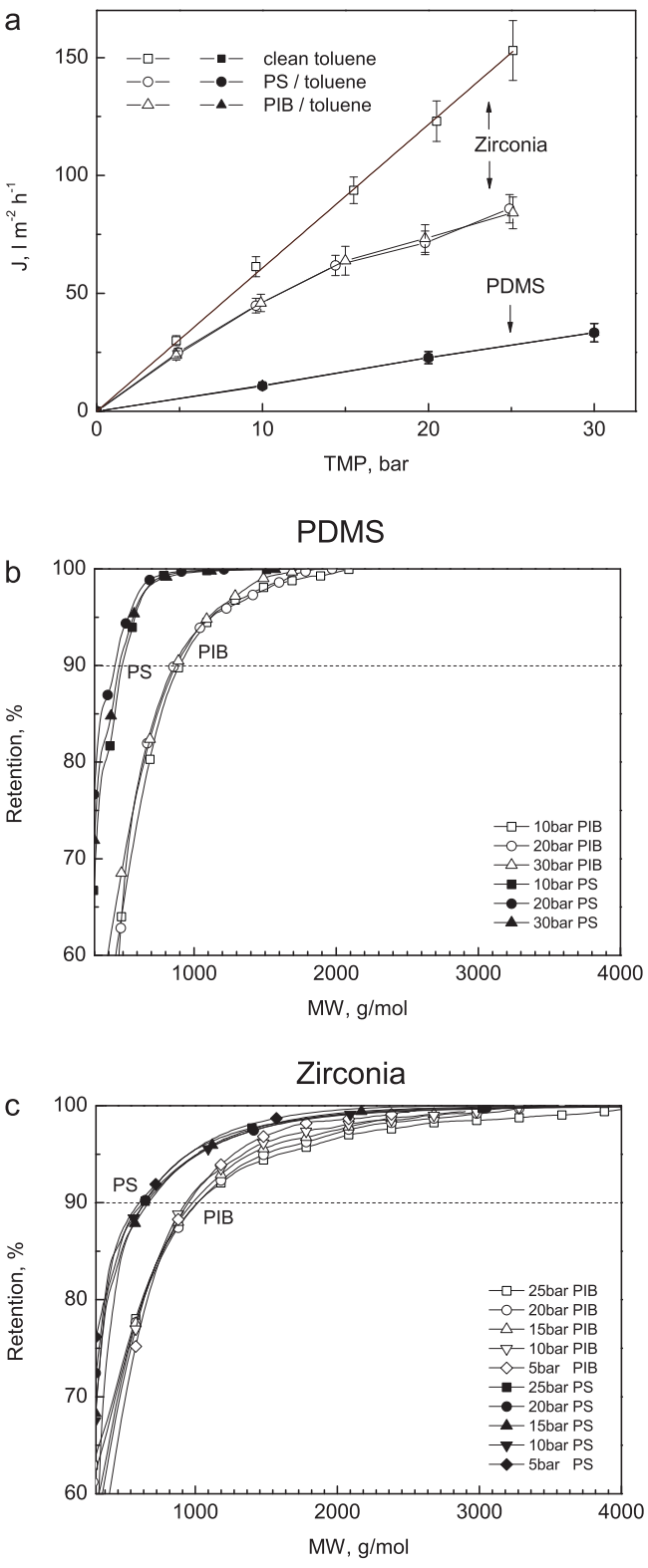


**Fig. 3.** Transport properties of the zirconia and PDMS membranes. (a) Flux of toluene, PIB/toluene and PS/toluene as a function of transmembrane pressure. Retention curves of PIB and PS in toluene for (b) composite PDMS hollow fiber membrane (c) zirconia $TiO_2$ multichannel membrane. In b and c the depicted symbols present an optical guide to distinguish between the experimental curves derived from the GPC analysis.

**Table 2**
Properties of solvents and solutes.

| | PIB | PS |
|---|---|---|
| Static stiffness parameter $\lambda^{-1}$, nm [31] | 1.27 | 2.35 |
| Chain diameter $d_b$, nm [31] | 0.64 | 1.01 |
| Radius of gyration, nm [32,33] | MW = 854 (n-heptane) 0.79 | MW = 904 (toluene) 0.598 |

the low solute concentration (0.3%, w/w). Stafie et al. investigated retention of oil in n-hexane by a PDMS/PAN composite membrane and reported an increase in retention with flux increase, at higher oil concentrations. The change of retention with flux was reduced at lower oil concentrations and was negligible below 8% (w/w) oil in n-hexane. In this work we used 0.3% (w/w) concentration of oligomers.

For the PDMS composite membrane, pressure independent solute retention combined with the linear relation between the flux and the pressure indicate that concentration polarization derived effects are not relevant. A quantitative analysis of concentration polarization is complicated by the uncontrolled turbulent hydrodynamics in the membrane module and the vibrations of the fiber. However, a relatively high mass transfer coefficient can be expected which combined with a low membrane flux corresponds to a rather small Peclet number. This indicates that the difference in concentration of oligomers in the liquid bulk and at the membrane surface will only be small.

The pure toluene flux through the porous zirconia increases linearly with pressure (Fig. 3a). Its permeance ($6.1 \pm 0.1$, $\mathrm{l\,m^{-2}\,h^{-1}\,bar^{-1}}$) is much higher as compared to the PDMS composite membrane. In the presence of PIB or PS the permeance is not constant anymore but decreases with increasing pressure and recovers slowly with decreasing pressure. This non-linear relation between flux and pressure can be indicative of concentration polarization derived effects. For this system the concentration polarization modulus was calculated according to [36]:

$$\frac{c_{i0}}{c_{ib}} = \frac{\exp(J_v\delta/D_i)}{1 + E_0[\exp(J_v\delta/D_i) - 1]} \quad (1)$$

and found to be approximately 11, whereas the Peclet number is ~2 ($\mathrm{Pe_{PS/toluene}} \approx \mathrm{Pe_{PIB/toluene}} \approx 2$), indicating that there is moderate enhancement in concentration of oligomers at the surface of the membrane and low osmotic pressure difference ($\Delta\Pi < 1$ bar). The non-linear relation is probably due to the presence of oligomers in the membrane pores, hindering the transport through the membrane. This also complies with the relatively long time (~hours) required for recovery of the permeability. In order to restore the flux to its original behavior only permeation with pure solvent was used. In the experiments no influence of the history of the experiments was found, which is a strong indication that fouling or irreversible phenomena did not occur.

The PS retention curves for the zirconia membrane reveal MWCO of 650 g/mol (Fig. 3c), in agreement with the specifications given by the manufacturer. The MWCO obtained with PIB (950 g/mol) is much higher. The lower PIB retention is probably due to its shape and flexibility: the thinner and more flexible PIB passes easier through the pores than the more rigid PS. Interestingly, the retention curves of PIB show a slight dependence on the pressure; for higher pressures a lower retention is observed. The reduced retention cannot be related to concentration polarization in a straightforward manner, because this phenomenon would in fact be more pronounced for the PS molecules (similar Peclet number, higher retention). The lower retention at higher pressures may indicate shear-induced deformation of the PIB molecules, allowing higher transport rate of these oligomers through the rigid pores. This effect will be unimportant for the rigid, non-deformable PS molecules.

### 3.2.2. Effect of solvent

This section deals with the influence of the solvent on the rejection of the PIB oligomers. Due to very limited solubility of PS in n-hexane, retention measurements could not be performed for PS/hexane.

Fig. 4a depicts the fluxes of pure hexane and a PIB/hexane mixture for both membranes. The general trends are the same as in the case of toluene (compare with Fig. 3). For the PDMS composite membrane, the flux of pure n-hexane and the PIB/n-hexane mixture are similar, and linearly proportional to the pressure. Despite comparable swelling of the membrane in toluene and n-hexane ($\Phi_{v/v} = 0.73$–$0.77$ [26]) the flux of n-hexane is much higher as compared to toluene. The permeance coefficient is sufficiently low ($P_{tol} = 1.8 \pm 0.1$, $\mathrm{l\,m^{-2}\,h^{-1}\,bar^{-1}}$) to assume that concentration polarization effects are negligible. Fig. 4b depicts the PIB retention curves of the PDMS membrane using toluene or n-hexane as solvent. For both solvents the PIB retention is almost independent of pressure. The MWCO of PIB in toluene is much higher (900 g/mol) than in n-hexane (650 g/mol). The main reason for the difference in MWCO is the higher permeance of n-hexane, resulting in a lower concentration of PIB in the permeate. These observations suggest that there is no direct coupling between the fluxes of solvent and solute.

For the zirconia porous membrane the flux of pure hexane increases linearly with transmembrane pressure (Fig. 4a). The permeance coefficient ($17.2 \pm 0.3$, $\mathrm{l\,m^{-2}\,h^{-1}\,bar^{-1}}$) is much larger than that of toluene. The presence of PIB results in a non-linear relation between flux and pressure, in fact at higher pressures the membrane permeance decreases with increasing pressure. Also in this case, the estimated Peclet number is ~3 [36] and the osmotic pressure difference is low ($\Delta\Pi < 2$ bar) indicating that concentration polarization induced osmotic effects cannot explain the drop in permeance. Similarly in this case, presence of PIB molecules in the pores seems to obstruct the flow. The retention of PIB by the zirconia membrane in the two solvents is in contrast with that of PDMS (Fig. 4c). The MWCO obtained with PIB in toluene is much lower (950 g/mol) than in n-hexane (higher than 1200 g/mol). Notably, the retention curves in n-hexane show a very pronounced pressure dependence. At high pressures the retention initially increases with MW until a maximum value and then decreases (see Fig. 4c). The initial increase in retention corresponds to enhanced size exclusion of larger molecules. The decrease in retention with MW for the larger molecules is typically attributed to concentration polarization and it is reversible. The effect can be estimated calculating the concentration polarization modulus as a function of MW. It shows in particular that larger molecules diffuse at a lower rate from the membrane surface back to the liquid bulk, causing an increase of high-MW PIB concentration in the boundary layer. A higher concentration gradient of large oligomers over the membrane surface results in higher flux of these molecules through the membrane and hence a lower retention. Superimposed effects can be an increase of the partitioning coefficient of the high MW oligomers [37] and the shear induced deformation of PIB molecules in the pores, similar to that reported by Beerlage et al. for polyimide UF membranes with ethyl acetate/high MW polystyrene (96 kg/mol) [25]. As suggested by Beerlage, a higher trans-membrane pressure, and corresponding larger flow through the pore, increases the frictional force on the solute molecules. The enhanced frictional force causes the polymer coil to unroll into more elongated conformations, which are smaller than the original polymer coil and pass through the pores more easily. It should be noted that in the present study the higher flux of n-hexane is due to the lower viscosity, and in a macroscopic description of the flow the shear forces inside the

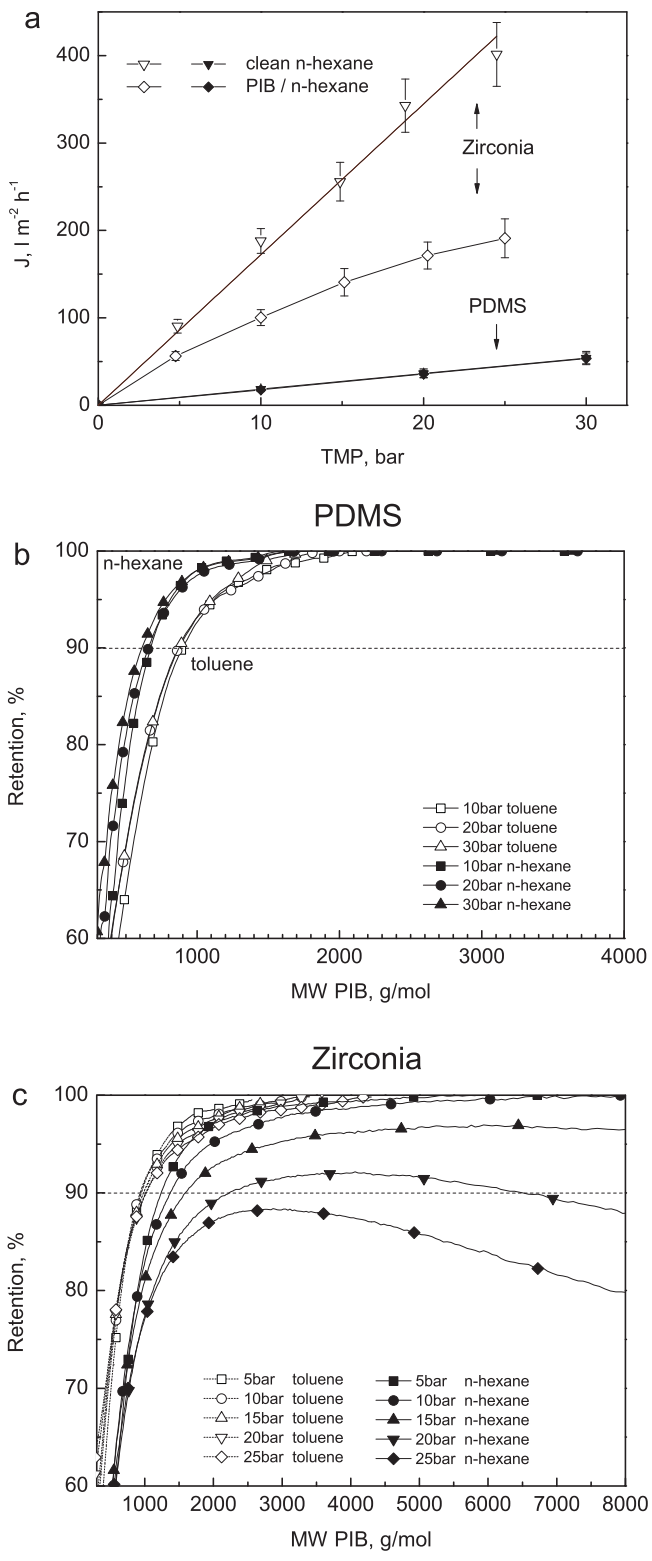


**Fig. 4.** Transport properties of the zirconia and PDMS membranes. (a) Flux of n-hexane and PIB/n-hexane as a function of transmembrane pressure. (b) Retention curves of PIB for PDMS. Solvents: toluene and n-hexane. (c) Retention curves of PIB for zirconia membrane. Solvents: toluene and n-hexane. In b and c the depicted symbols present an optical guide to distinguish between the experimental curves derived from the GPC analysis.

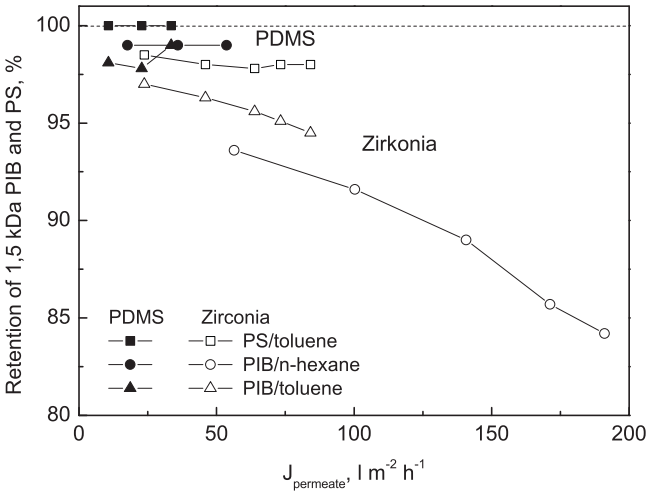


**Fig. 5.** Retention of 1500 g/mol rigid PS and flexible PIB by the PDMS (full symbols) and zirconia (open symbols) membranes. Solvents: n-hexane and toluene.

liquid would remain unchanged for a given pressure drop. However, given the comparable nanometer scale dimensions of the pores and oligomers, for the system under study such a macroscopic description is probably not valid.

Finally, it is important to point out that all experiments were carried out on the same membranes in order to exclude batch-differences. After all permeation experiments, filtration of PS/toluene was repeated for both membranes. The behavior of the membranes was checked for hysteresis between the different pressures and solutions. No significant changes in retention were observed in comparison to the initial results suggesting that the membrane transport properties were not compromised during the study. The fluxes of the membranes changed but could be restored in time with normal permeation and no evidence of fouling was observed during the tests.

## 4. Conclusions

To summarize our observations, Fig. 5 shows the retention of 1500 g/mol PS and PIB as a function of total permeate flux for the dense rubber PDMS membrane and the rigid porous zirconia membrane.

In the case of the PDMS composite membrane there is very little effect of flux on retention. For this membrane the solvent and solute are transported independently through the membrane and solvent–membrane and solute–membrane determine retention behavior. For the zirconia membrane the retention of flexible PIB decreases dramatically at higher fluxes, whereas retention of the more rigid PS stays relatively constant. For this porous membrane there is direct coupling between the solvent and solute fluxes and the superimposed effects concentration polarization and shear induced solute deformation are considerable. The presented observations point out that the selection of the proper solvent–solute system and the process conditions for the MWCO determination as well as the interpretation of MWCO data in organic solvents requires extreme caution.

## Acknowledgments

We would like to gratefully acknowledge the Dutch Technology Foundation (STW) (Project No. 07349) for the financial support. The authors also would like to thank Nadia Vleugels and Lydia Bolhuis-Versteeg for the help with permeation measurements and Clemens Padberg for the help with GPC analysis.

## References


[1] Y.H. See Toh, F.W. Lim, A.G. Livingston, Polymeric membranes for nanofiltration in polar aprotic solvents, J. Membr. Sci. 301 (2007) 3–10.
[2] K. Vanherck, P. Vandezande, S.O. Aldea, I.F.J. Vankelecom, Cross-linked polyimide membranes for solvent resistant nanofiltration in aprotic solvents, J. Membr. Sci. 320 (2008) 468–476.
[3] L.S. White, C.R. Wildemuth, Aromatics enrichment in refinery streams using hyperfiltration, Ind. Eng. Chem. Res. 45 (2006) 9136–9143.
[4] J.P. Sheth, Y. Qin, K.K. Sirkar, B.C. Baltzis, Nanofiltration-based diafiltration process for solvent exchange in pharmaceutical manufacturing, J. Membr. Sci. 211 (2003) 251–261.
[5] J.T. Scarpello, D. Nair, L.M. Freitas dos Santos, L.S. White, A.G. Livingston, The separation of homogeneous organometallic catalysts using solvent resistant nanofiltration, J. Membr. Sci. 203 (2002) 71–85.
[6] A. Livingston, L. Peeva, S. Han, D. Nair, S.S. Luthra, L.S. White, L.M. Freitas Dos Santos, Membrane separation in green chemical processing, Ann. N. Y. Acad. Sci. 984 (2003) 123–141.
[7] S.S. Luthra, X. Yang, L.M. Freitas dos Santos, L.S. White, A.G. Livingston, Homogeneous phase transfer catalyst recovery and re-use using solvent resistant membranes, J. Membr. Sci. 201 (2002) 65–75.
[8] V. Kale, S.P.R. Katikaneni, M. Cheryan, Deacidifying rice bran oil by solvent extraction and membrane technology, J. Am. Oil Chem. Soc. 76 (1999) 723–727.
[9] H.J. Zwijnenberg, A.M. Krosse, K. Ebert, K.V. Peinemann, F.P. Cuperus, Acetone-stable nanofiltration membranes in deacidifying vegetable oil, J. Am. Oil Chem. Soc. 76 (1999) 83–87.
[10] J.C.T. Lin, A.G. Livingston, Nanofiltration membrane cascade for continuous solvent exchange, Chem. Eng. Sci. 62 (2007) 2728–2736.
[11] D. Shi, Y. Kong, J. Yu, Y. Wang, J. Yang, Separation performance of polyimide nanofiltration membranes for concentrating spiramycin extract, Desalination 191 (2006) 309–317.
[12] P. Vandezande, L.E.M. Gevers, I.F.J. Vankelecom, Solvent resistant nanofiltration: separating on a molecular level, Chem. Soc. Rev. 37 (2008) 365–405.
[13] J.A. Whu, B.C. Baltzis, K.K. Sirkar, Nanofiltration studies of larger organic microsolutes in methanol solutions, J. Membr. Sci. 170 (2000) 159–172.
[14] D. Bhanushali, S. Kloos, D. Bhattacharyya, Solute transport in solvent-resistant nanofiltration membranes for non-aqueous systems: experimental results and the role of solute–solvent coupling, J. Membr. Sci. 208 (2002) 343–359.
[15] D. Bhanushali, S. Kloos, C. Kurth, D. Bhattacharyya, Performance of solvent-resistant membranes for non-aqueous systems: solvent permeation results and modelling, J. Membr. Sci. 189 (2001) 1–21.
[16] N. Stafie, D.F. Stamatialis, M. Wessling, Insight into the transport of hexane–solute systems through tailor-made composite membranes, J. Membr. Sci. 228 (2004) 103–116.
[17] N. Stafie, D.F. Stamatialis, M. Wessling, Effect of PDMS cross-linking degree on the permeation performance of PAN/PDMS composite nanofiltration membranes, Sep. Purif. Technol. 45 (2005) 220–231.
[18] D.F. Stamatialis, N. Stafie, K. Buadu, M. Hempenius, M. Wessling, Observations on the permeation performance of solvent resistant nanofiltration membranes, J. Membr. Sci. 279 (2006) 424–433.
[19] A.V. Volkov, D.F. Stamatialis, V.S. Khotimsky, V.V. Volkov, M. Wessling, N.A. Plate, Poly[1-(trimethylsilyl)-1-propyne] as a solvent resistance nanofiltration membrane material, J. Membr. Sci. 281 (2006) 351–357.
[20] S. Darvishmanesh, J. Degrève, B. Van Der Bruggen, Mechanisms of solute rejection in solvent resistant nanofiltration: the effect of solvent on solute rejection, Phys. Chem. Chem. Phys. 12 (2010) 13333–13342.
[21] P.P.I. Voigt, T. Holborn, G. Dudziak, M. Mutter, A. Nickel, Ceramic nanofiltration membranes for applications in organic solvents, in: 9th Aachen Membrane Colloquium, Aachen, Germany, 2003, pp. OP 20-21–OP 20-11.
[22] H.J. Zwijnenberg, A standardized characterization method for solvent resistant nanofiltration membrane modules, in: International Congress on Membranes 2005, Seoul, Korea, 2005, Fr12B-3I-481.
[23] Y.H. See Toh, X.X. Loh, K. Li, A. Bismarck, A.G. Livingston, In search of a standard method for the characterisation of organic solvent nanofiltration membranes, J. Membr. Sci. 291 (2007) 120–125.
[24] S.M. Dutczak, M.W.J. Luiten-Olieman, H.J. Zwijnenberg, L.A.M. Bolhuis-Versteeg, L. Winnubst, M.A. Hempenius, N.E. Benes, M. Wessling, D. Stamatialis, Composite capillary membrane for solvent resistant nanofiltration, J. Membr. Sci. 372 (2011) 182–190.
[25] M.A.M. Beerlage, M.L. Heijnen, M.H.V. Mulder, C.A. Smolders, H. Strathmann, Non-aqueous retention measurements: ultrafiltration behaviour of polystyrene solutions and colloidal silver particles, J. Membr. Sci. 113 (1996) 259–273.
[26] N. Stafie, Poly(dimethyl siloxane)-based composite nanofiltration membranes for non-aqueous applications, Ph.D. Thesis, University of Twente, Enschede, The Netherlands, 2004.
[27] A.P. Sokolov, V.N. Novikov, Y. Ding, Why many polymers are so fragile, J. Phys.: Condens. Matter 19 (2007), 205116/1–205116/8.
[28] J. De Jong, N.E. Benes, G.H. Koops, M. Wessling, Towards single step production of multi-layer inorganic hollow fibers, J. Membr. Sci. 239 (2004) 265–269.
[29] H.-G. Elias, An Introduction to Plastics, Wiley-VCH, Weinheim, 2003.
[30] J.E. Mark, Polymer Data Handbook, Oxford University Press, Inc., Oxford, 1999.
[31] F. Abe, Y. Einaga, H. Yamakawa, Intrinsic viscosity of oligo- and polyisobutylenes: treatments of negative intrinsic viscosities, Macromolecules 24 (1991) 4423–4428.
[32] M. Yamada, M. Osa, T. Yoshizaki, H. Yamakawa, Excluded-volume effects on the mean-square radius of gyration of oligo- and polyisobutylenes in dilute solution, Macromolecules 30 (1997) 7166–7170.
[33] F. Abe, Y. Einaga, T. Yoshizaki, H. Yamakawa, Excluded-volume effects on the mean-square radius of gyration of oligo- and polystyrenes in dilute solutions, Macromolecules 26 (1993) 1884–1890.
[34] J.P. Robinson, E.S. Tarleton, K. Ebert, C.R. Millington, A. Nijmeijer, Influence of cross-linking and process parameters on the separation performance of poly(dimethylsiloxane) nanofiltration membranes, Ind. Eng. Chem. Res. 44 (2005) 3238–3248.
[35] E.S. Tarleton, J.P. Robinson, C.R. Millington, A. Nijmeijer, Non-aqueous nanofiltration: solute rejection in low-polarity binary systems, J. Membr. Sci. 252 (2005) 123–131.
[36] R. Baker, Membrane Technology and Applications, 2nd ed., John Wiley & Sons, Ltd., 2004.
[37] I. Teraoka, Polymer solutions in confining geometries, Prog. Polym. Sci. 21 (1996) 89–149.